57

Compressed Sensing Prototype for Flexible Wireless System

Doohwan Lee, Takayuki Yamada, Hiroyuki Shiba, Kazunori Akabane,
Yo Yamaguchi, Takana Kaho, and Kazuhiro Uehara
NTT Network Innovation Laboratories, NTT Corporation
E-mail: lee.doohwan@lab.ntt.co.jp

Abstract

Compressed sensing is recently developed technology which directly compresses sparse data with the sub-Nyquist rate information. It can be considered as finding a solution of an ill-posed inverse problem of the sparse data. The introduction of recent trends and achievements of compressed sensing including the structured compressed sensing and 1-bit compressed sensing will be given for the comprehensive understanding in this paper. Flexible wireless system is a unified wireless platform composed of flexible access points and a flexible signal processing unit. The goal of a flexible access system is the provision of a unified wireless platform which has the capability of receiving various types of wireless signals regardless of their signal type. By transferring whole wireless signal data through a wired access line, various types of wireless signals are processed at flexible access points. We implemented a prototype of flexible wireless system in which compressed sensing is used as a radio wave compression method. This paper also introduces flexible wireless system prototype implemented using compressed sensing technology.

1. Compressed Sensing

Since the seminal work of Donoho [1] and Candes [2], interest in compressed sensing technology has been explosively growing. A plethora of research regarding compressed sensing has taken place from the theory to the applications [3]. Numerous numbers of research works and projects are also currently ongoing in various fields including astronomy, photonics, or signal processing [4-6]. Although several introductive materials have been published [2, 7-8], readers still feel difficulties in understanding compressed sensing technology. This is due to the fact that compressed sensing was born by combining various fields such as mathematics, information theory, signal processing, and probability theory. To provide the comprehensible explanations

to the readers, this paper firstly describes the basic and introduction to compressed sensing.

Let $N \times 1$ signal vector $\mathbf{X}$ be sparsely represented with an $N \times N$ basis matrix Ψ and $N \times 1$ sparse vector $\mathbf{s}$ as $\mathbf{X} = \Psi\mathbf{s}$. It follows that $K \times 1$ measurement vector $\mathbf{Y}$ is obtained from $K \times N$ matrix measurement matrix Φ as $\mathbf{Y} = \Phi\mathbf{X} = \Phi\Psi\mathbf{s}$. By replacing $\Phi\Psi$ with Θ, the equivalent notation $\mathbf{Y} = \Theta\mathbf{s}$ I s obtained. Typically, the inverse problem $\mathbf{s} = \Theta^{-1}\mathbf{Y}$ is ill-posed and not solvable (NP-hard). However, compressed sensing theory proved that this inverse problem can be solvable with overwhelming probability when $\mathbf{s}$ is sparse, and Θ satisfies restricted isometry properly (RIP, description will be followed) by cast the ill-posed inverse problem to l1-norm minimization problem.

$$\min\|\tilde{\mathbf{s}}\|_1 \text{ subject to } \mathbf{Y} = \Theta\tilde{\mathbf{s}} \text{ and } \tilde{\mathbf{s}} \in \mathbf{R}^n,$$

where, $\|\tilde{\mathbf{s}}\|_1 = \sum_i |\tilde{s}_i|$ and $\mathbf{R}^n$ is the set of $N \times 1$ vector.

This l1-norm minimization problem is solvable by basis pursuit [9], the iterative greedy algorithm [10], or other similar algorithms.

Above stated RIP provides the sufficient condition of measurement matrix Φ and basis matrix Ψ for solving the l1-norm minimization problem [11-12]. When compressed sensing matrix Θ $(= \Phi\Psi)$ satisfies the following inequality for all S-sparse vectors, matrix Φ is said to obey the RIP of order S.

$$(1-\delta)\|\mathbf{s}\|_2^2 \leq \|\Theta\mathbf{s}\|_2^2 \leq (1+\delta)\|\mathbf{s}\|_2^2,$$

where, $\|\mathbf{s}\|_2 = \sum_i s_i^2$ and $\delta (0 \leq \delta < 1)$ is the smallest constant that satisfies above equation. This l1-norm minimization problem is solvable by the linear programming, which is one of the well established convex optimization methods, with practical complexity $O(n^3)$ [9, 11].

In the geometrical sense, the Euclidian distance between any two S-sparse vectors in $\mathbf{R}^n$ is approximately preserved after projection when Φ obeys the RIP of order S with δ.

Figure 1 illustrates how l1-norm minimization method finds the sparse solution. L1-norm minimization method finds the solution from the infinite solution plane by adjusting (optimizing) l1-ball ($\|\tilde{\mathbf{s}}\|_1$). As confirmed from the figure, the solution obtained by adjusting l1-ball is inherently sparse (this statement is true only when RIP is satisfied. Detailed explains will be followed). On the other hand, l2-norm minimization method (minimizing mean square error) does not yield the sparse solution because the point where l2-ball ($\|\tilde{\mathbf{s}}\|_2$) reach the solution plane is usually non sparse point. This explains why and how
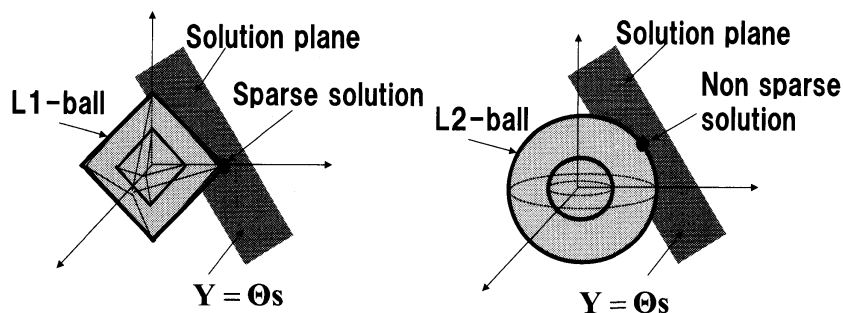
(a) L1-norm minimization   (b) L2-norm minimization

Fig. 1 Graphical illustration of l1-norm minimization and l2-norm minimization method.

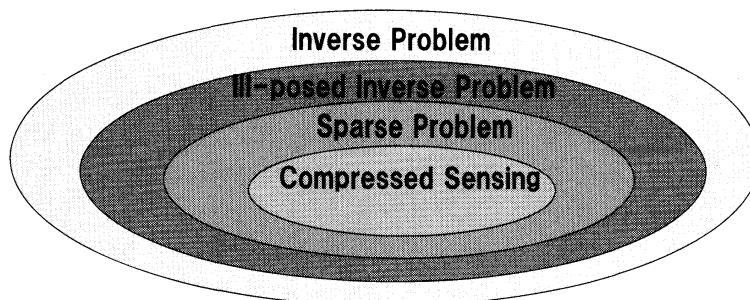| Ill-posed Inverse Problem			
	Sparse assumption		
			Compressed sensing
Non-solvable	Solvable but NP hard		Practically solvable

Fig. 2 Positioning of compressed sensing in the framework of inverse problem.

l1-norm minimization is used for compressed sensing.

Figure 2 summarizes the positioning of compressed sensing in the framework of inverse problem. Ill-posed inverse problem is usually non-solvable. Although it is solvable when the solution is sparse, it is still NP-hard and impractical. However, when compressed sensing is taken into consideration, the ill-posed inverse problem with sparse solution can be solvable with practical complexity $O(n^3)$ [9, 11].

L1-norm minimization does not always guarantee finding the sparse solution. One of the core contributions of research work on compressed sensing is the proof that RIP guarantees finding sparse solution with overwhelming probability.

Figure 3 illustrates the concept of RIP when R^3 vector is projected onto R^2 (ill-posed inverse problem formed by 2 equations and 3 variables). When RIP is satisfied, the Euclidean distance of two sparse vectors are properly maintained.

(a) L1-norm minimization   (b) L2-norm minimization

Fig. 3 Graphical illustration of RIP.
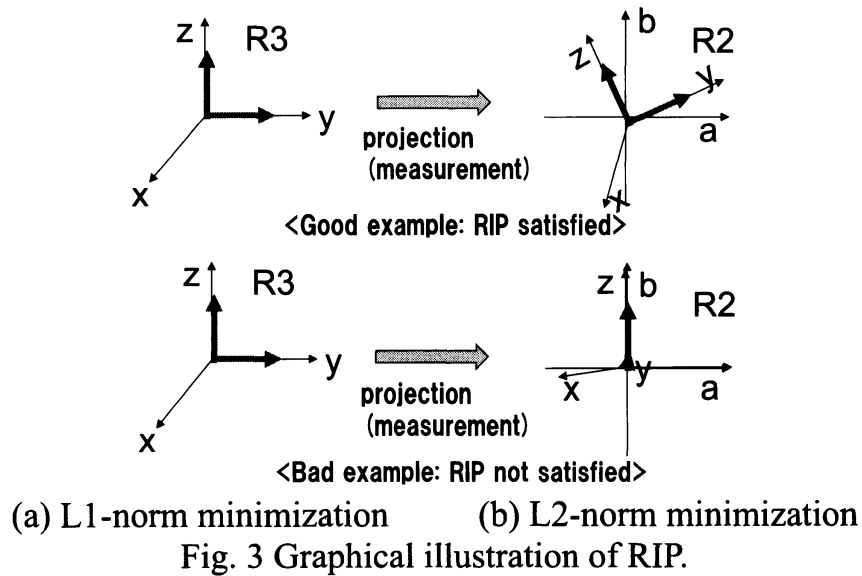
Therefore, information in the high dimension (R^3 in the figure) is not lost in the low dimension (R^2 in the figure), which provides the possibility of reconstruction of original high dimensional information from the low dimensional information. On the other hand, when RIP is not satisfied, the Euclidean distance of two sparse vectors are not maintained, and some information is lost. Consequently, it is not possible to reconstruct the original high dimensional information.

2. Structured Compressed Sensing

Difficulties in hardware implementation and expensive calculation cost of complete random measurement matrices motivated the usage of the structured matrices as the measurement matrices. Two such promising candidates are Toeplitz matrix (T) and circulant matrix (C). Measurement by Toeplitz matrices and circulant matrices are realized by the linear convolution and the circular convolution, respectively. In terms of the causality of the physical signal, Toeplitz matrices are suitable for practical hardware implementations [13-15]. In case of the circular matrices, however, the additional effort is necessary due to the noncausality caused by the circular convolution.

As discussed in the previous section, this paper exclusively consider the digital compressed sensing and applies circulant matrices to save the calculation cost because 1) the noncausality problem is relaxed in the digital compressed sensing, and 2) matrix operations of the circular matrices are simpler than Toeplitz matrices.

Measurement matrix in this paper is generated by the partial random circular matrix as $\Phi = RC = RUDU^*$. R is a $N \times M$ matrix ($N < M$) consist of partial

rows of the $M \times M$ identity matrix. **C** is $M \times M$ random circulant matrix of which first row consist of $M \times 1$ random numbers and every left-to-right descending diagonal is constant. U and U^* are the FFT and IFFT matrices of which size are $M \times M$, respectively. **D** is a $M \times M$ diagonal matrix with diagonal elements is generated by DFT of the first row of **C** Therefore, calculation cost of partial random circulant measurement matrices are $O(2MlogM+M)$ including FFT, IFFT, and diagonal matrix multiplication operation, which is much lower than that of the complete random measurement matrix, $O(NM)$.

Due to the decreased degrees of the freedom, increased number of measurements is necessary when partial random circulant matrices are used. It has been proven that if **R** is the randomly selected rows of the identity matrix and **C** is generated by Rademacher variables, $O(K^{1.5}log^{1.5}M)$ measurements satisfies RIP in many reconstruction algorithms [16]. Although this is larger than the case of the benchmark result given by $O(Klog(M/K))$, our empirical observations for the spectrum sensing showed that the partial random circulant matrices work as efficient as the complete random matrices.

3. 1-bit Compressed Sensing

Increased communication cost caused by the quantization, particularly in networked system, motivates us to use 1-bit compressed sensing.

Boufounous [17] firstly proposed 1-bit compressed sensing, which only extracts sign data from measured data, $Y = sign(\Theta s)$, and reconstructs the original signal from the extracted sign data. Although the amplitude information is lost during the measurement stage, [17] showed the possibility of the reconstruction. Reconstruction method proposed in [17] solved the sparse signal inversion problem by enforcing the solution $(\tilde{s})$ lies on the unit sphere to artificially resolve the amplitude ambiguity as bellows.

$$\min \|\tilde{s}\|_1 \text{ subject to } Y = sign(\Theta s), \|s\|_2 = 1, \text{ and } \tilde{s} \in R^M.$$

In the geometric perspective, the surface of the unit sphere and Rows of Θ represent the collections of all $M \times 1$ signal vectors bereft of amplitude information and intersection planes of the unit sphere, respectively. Note that plenty of intersection planes with different directions and their sign information can specify the specific area of the surface of the unit sphere. If $M \times 1$ signal vectors are K-sparse, their location on the surface of the unit sphere can be exactly specified provided that the numbers of intersection planes are plenty enough. Jacques [18] provides the theoretical analysis on the best achievable performance of 1-bit compressed sensing by introducing the $B\varepsilon SE$ which is defined by

$$d_S(\mathbf{X_1}, \mathbf{X_2}) - \varepsilon \leq d_H\big(sign(\Phi \mathbf{X_1}) - sign(\Phi \mathbf{X_2})\big) \leq d_S(\mathbf{X_1}, \mathbf{X_2}) + \varepsilon,$$
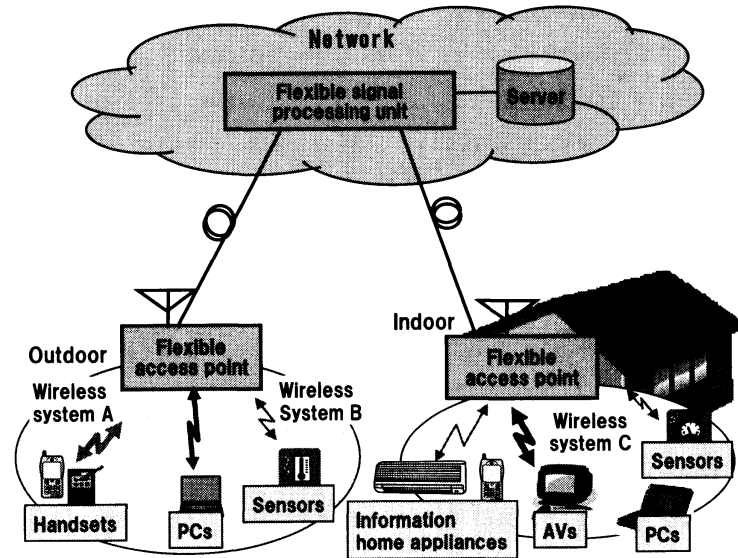
Fig.4 Concept of a flexible wireless system.

where $d_S (0 \le d_S \le 1)$ is the normalized angle between two $M \times 1$ vectors and $d_H (0 \le d_H \le 1)$ is the normalized hamming distance between two $N \times 1$ sign vectors, respectively. $\varepsilon (0 \le \varepsilon < 1)$ is the smallest constant that satisfies above equation.

Similarities of BεSE and RIP provide the brilliant geometric intuition to comprehend how reconstruction of 1-bit compressed sensing is guaranteed. The Euclidean distances between two $M \times 1$ vectors and two $N \times 1$ measured vectors correspond to the normalized angle between two $M \times 1$ amplitude-bereft vectors and the hamming distance between two $N \times 1$ sign vectors, respectively. Therefore, BεSE guarantees the preservation of the angle between two amplitude-bereft vectors in $\mathbf{R}^M$ likewise the δ-stable embedding in the conventional compressed sensing. [18] showed that $O(K\log(M))$ measurement satisfies BεSE when the complete Gaussian random measurement matrices are used. Theoretical guarantee of BεSE with structured random measurement matrices has not yet been investigated in the literature.

4. Flexible Wireless System

Rapid developments and changes of wireless radio environments require a unified platform which can flexibly deal with various wireless radio systems. To satisfy this requirement, we have proposed a flexible wireless system (FWS) [19].

Figure 4 illustrates the concept of the FWS. Various wireless signals are simultaneously received by flexible access points. Flexible access points have the capability of receiving a wide variety of wireless signals from several

hundred megahertz to several gigahertz. The received radio wave data is transferred to the flexible signal processing unit through the broadband wired access line. The flexible signal processing unit performs multiple types of signal analysis by software exploiting software defined radio and cognitive radio technologies [20].

The FWS consists of three key technologies: 1) RF technology for reception and transmission over wide frequency bands, 2) data compression technology between flexible access points and flexible signal processing unit, and 3) signal processing technology for extracting the desired signal from overlapped and interfered signals.

RF and signal processing technologies were implemented by FWS prototype [21]. The broadband low noise amplifier with wide dynamic range [22] and signal separation method for overlapped signals were implemented. The experiment results of the FWS prototype confirmed the system's practicality. The front-end ICs for receiver yielded the signal reception capability from 300 MHz to 3 GHz frequency bands signals. The signal processing unit also yielded the capability of demodulating the overlapped signal by software with reduced CPU processing load. These RF and signal processing technologies are further expanded to [23] and [24], respectively.

We have recently developed the updated FWS prototype. Data compression technology between flexible access points and flexible signal processing unit is mainly concerned in the second generation FWS prototype. To overcome the huge bandwidth necessity for transferring the radio wave data, recently developed compressed sensing technology [1, 3] is applied as a data compression method. Moreover, to achieve the enhanced performance, our previous research works [19, 25-26] are also implemented. [19] proposed the combined Nyquist and compressed sampling method to apply compressed sensing technology for multiple signals with different priorities. [25] suggested the weighted compressed measurement matrix generation method for utilizing the prior information. [26] developed the processing burden reduction method using averaged compressed sensing.

5. Implementation of Flexible Wireless System Prototype using Compressed Sensing

5. 1 Architecture of Prototype

Figure 5 shows the architecture of the prototype. Flexible access point consists of RF front-end, ADC, DAC, compressed sensing unit, and IP packetizing (unpacketizing) unit. The wired access line is implemented by 10 Gbit/s optical fiber. Flexible signal processing unit consists of baseband signal processing unit, compressed sensing reconstruction unit, and IP packetizing (unpacketizing) unit. For the uplink signal processing, the received RF wireless signals at a flexible
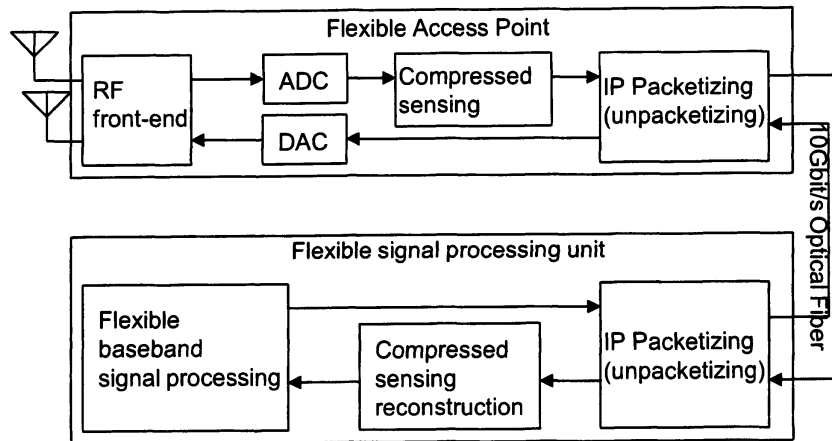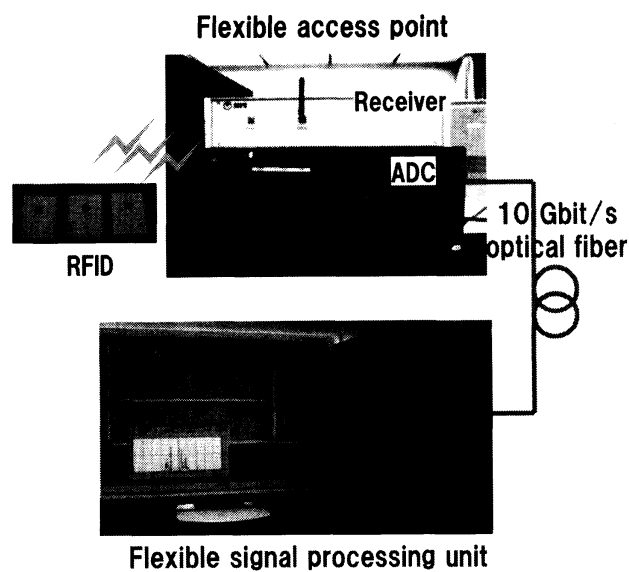
Fig.5 Architecture of the Prototype.

Fig.7 Appearance of the Prototype.

access point are downconverted into IF band after broadband low noise RF operation. These downconverted signals are compressed using compressed sensing technology after the analog-to-digital conversion. Then, the compressed signals are transferred to the flexible signal processing unit through the 10 Gbit/s optical fiber after the IP packetizing. Subsequently, the transferred compressed signals are reconstructed by compressed sensing reconstruction algorithm such as L1-mininization method after the IP unpacketizing. Finally, the baseband signal processing is conducted using the reconstructed signals by software. The downlink signal processing is conducted by opposite order except the compressed sensing and its reconstruction process. All signal processing is conducted by software except RF operation, ADC, and DAC. The appearance of the prototype (receiver part only) is shown in Fig. 6.
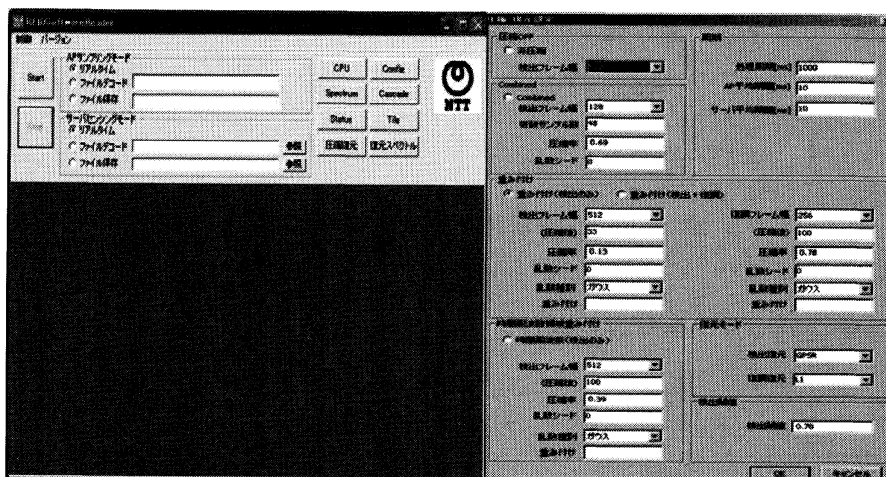
Fig. 8 User interface of flexible signal processing unit.

TABLE 1. EXPERIMENTS PARAMETERS

Bandwidth	10 MHz
Sampling rate	20 Msps
Quantization	16 bits (I/Q 32 bits)
Channel Bandwidth of RFID	~ 300 KHz
Modulation of RFID	FSK
Data rate of RFID	2.4 Kbit/s, 9.6 Kbit/s, 19.2 Kbit/s, 38.4 Kbit/s
Period of RFID	1 sec
Signal duration of RFID	5, 10, 20, 80 msec
Average Period	1 msec – 10 msec
Compression rate	0.0001 ~ 0.001

5. 2 Experiments

This section introduces some experimental results. All operations are controlled by software at the flexible signal processing unit. Figure 8 shows the user interface of flexible signal processing unit. It is implemented using Visual C++ and run on Window OS. All of parameter settings are done by control window at flexible signal processing unit. Control parameters necessary for RF and compressed sensing operations such as sampling rate, initial seed for random measurement matrix generation, period of average, and frame length are transferred from the flexible signal processing unit to the flexible access points. If necessary, updated control parameters are transferred as well.

Some important parameter settings for experiments are given in Table 1. The whole bandwidth 10 MHz is sampled at 20 Msps at flexible access point. Sampled data is compressed by the averaged compressed sensing and transferred
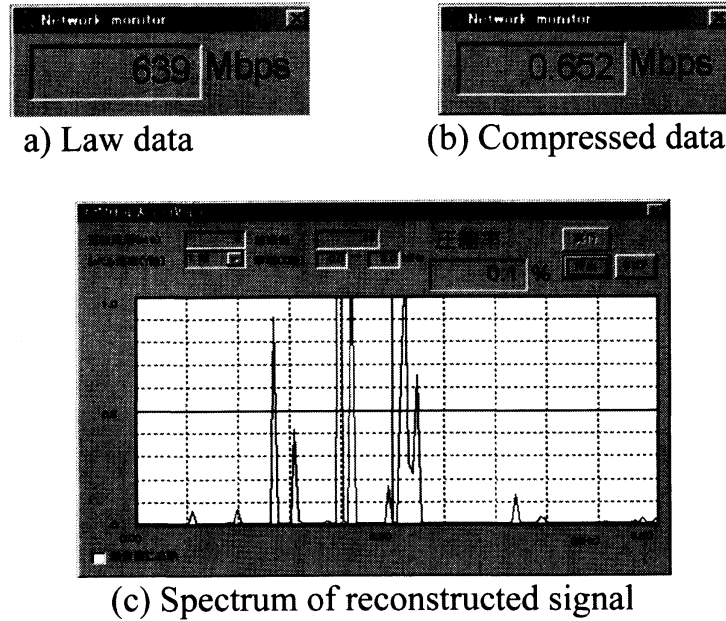
a) Law data   (b) Compressed data

(c) Spectrum of reconstructed signal

Fig. 9 Snapshots of transmitted data rate and reconstructed signal.

to flexible signal processing unit. The data rate of RFID is varied from 2.4 Kbit/s to 38.4 Kbit/s. Due to the spectral leakage, its channel bandwidth occupies up to 300 KHz. The frequency domain sparsity is 3% (300 KHz among 10 MHz). Signal duration of RFIDs varies from 5 to 80 msec, and their period is 1sec. Therefore, time domain sparsity is 0.5 to 8%. Average period is set from 1 to 10 msec. Of course, tradeoff between processing burden and time resolution exist depends on the length of average period. The channel between RFID tags and the distributed flexible access point was non-fading AWGN channel.

Figure 9 shows snapshots of operation of prototype. Figure 9(a) shows the law data when compressed sensing is not applied. For the transfer the 10 MHz radio wave without compression, 640 Mbit/s transfer rate is necessary. Figure 9(b) shows the data transfer rate when compressed sensing is applied. Almost compression rate of 0.001 is achieved in this example. Figure 9(c) shows the reconstructed signal with compressed data. It is confirmed that three RFID signals are clearly detected. Note that RFID signals are actually not overlapped in the time domain in this example. The reason what three RFID signals seems to exist together in Figure 9(c) is due to the update time of display, which is not related with compression or detection performance.

Figure 10 and 11 show experimental results to evaluate the performance of partial circulant measurement matrices, 1-bit compressed sensing, and block BIHT algorithm with various parameter settings. All curves of the detection success rate (P_d) are obtained with 0.01 of the detection false alarm rate (P_f). GPSR and binary iterative hard thresholding (BIHT) [18] are used as reconstruction algorithms for the conventional and 1-bit compressed sensing,
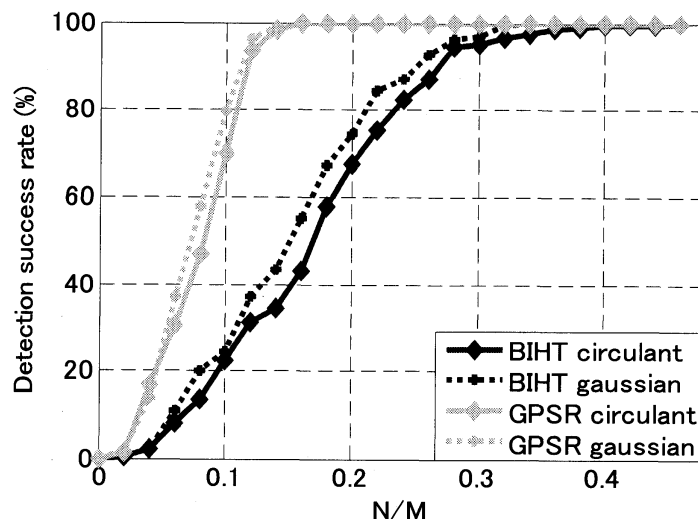
Fig.10 Detection success probability of the conventional and 1-bit CS in terms of frame compression rate.
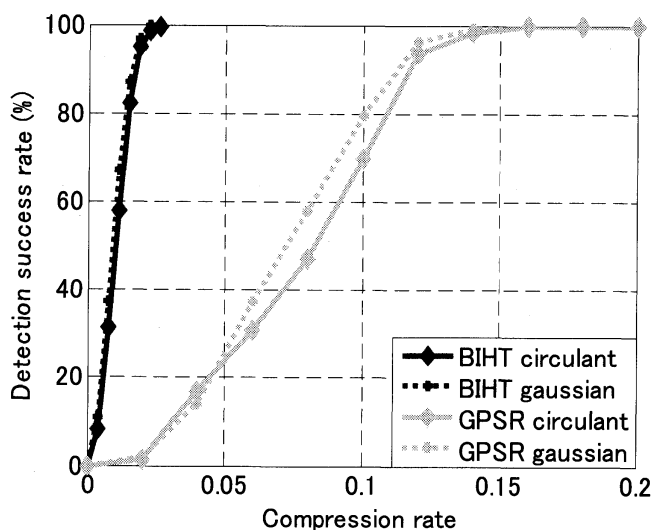

Fig.11 Detection success probability of the conventional and 1-bit CS in terms of whole compression rate.

respectively.

Figure 10 shows two comparisons: 1) complete random vs. partial random circulant measurement matrices and 2) conventional vs. 1-bit compressed sensing in terms of P_d. With respect to the first comparison, P_d of the partial random circulant matrices yield almost similar results with that of the complete random measurement matrices. Since the RIP is the sufficient condition, some empirical observations showed more favorable results than theoretical analysis. Spectrum sensing is also one of such cases. With respect to the second comparison, K/N for P_d over 0.99 are 0.14 and 0.4 in the conventional and 1-

bit compressed sensing, respectively. 1-bit compressed sensing needs larger number of measurements because it uses only sign information.

Figure 11 shows the same results of Fig. 1 in terms of the total compression rate including quantization effect. Note that curves of 1-bit compressed sensing are shifted to left and compression rate at 0.025 yields P_d over 0.99. This proves that 1-bit compressed sensing can save communication cost for spectrum sensing in networked system.

5. Conclusion

This paper provided the basic and intuitive introduction to compressed sensing. Compressed sensing is a new technology which utilizes the inherent sparsity of the signal. It is a mathematically well proved and established technology, which may have the unlimited possibilities to be applied in various applications. To tackle calculation and communication cost problems caused by the completely random measurement matrices and quantization, this paper also introduces the structured compressed sensing and 1-bit compressed sensing. Calculation cost of partial random circulant measurement matrices is reduced to O(2MlogM+M) using the property of the circulant matrices. Finally, this paper provides some experimental results. Experimental results showed that the partial random circulant matrices work as efficient as completely random measurement despite the reduced degrees of freedom, and its performance can be greatly advanced by applying 1-bit compressed sensing.

Acknowledgment

References

[1]   D. Donoho, "Compressed sensing," IEEE Trans. Inf. Theory, Apr. 2006.
[2]   E. Candes and M. Wakin, "An introduction to compressive sampling," IEEE Signal Process., Mag., vol. 25, no. 2, pp.21-30, Mar, 2008.
[3]   Compressive sensing resources, [Online]. Available: http://dsp.rice.edu/cs.
[4]   J. Bobin and et al., "Compressed sensing in astronomy," IEEE J. Sel. Top. Sign. Process., vol. 2, no. 5, pp.718-726, Oct. 2008.
[5]   M. Lustig, D. Donoho, J. Santos, and J. Pauly, "Compressed sensing MRI," IEEE Signal Process, Mag., vol. 25, no. 2, pp.72-82, Mar, 2008.
[6]   M. Duarte, et al., "Single-pixel imaging via compressive sampling," IEEE Signal Process Mag., vol. 25, no. 2, pp.83-91, Mar, 2008.
[7]   R. Baraniuk, "Compressive sensing [Lecture notes]," IEEE Signal Process Mag., vol. 24, no. 4, pp. 118-121, Jul. 2007.

[8] M. Fornasier and H. Rauhut, Compressive sensing, In O. Scherzer, editor, Handbook of Mathematical Methods in Imaging, Springer to appear.

[9] E. Candes and J. Romberg, "l1-magic: Recovery of Sparse Signals via Convex Programming," [Online]: /www.l1-magic.org. Oct. 2005.

[10] J. Tropp and A. Gilbert, "Signal recovery from random measurement via orthogonal matching pursuit," IEEE Trans. Inf. Theory, Dec. 2007.

[11] E. Candes and T. Tao, "Decoding by linear programming," IEEE Trans. Inf. Theory, vol. 51, no. 12, pp. 4203-4215, Dec. 2005.

[12] E. Candes, J. Romberg, and T. Tao, "Robust uncertainty principles: Exact signal reconstruction from highly incomplete frequency information," IEEE Trans. Inf. Theory, vol. 52, no. 2, pp. 489-509, Feb. 2006.

[13] J. Haupt et al., "Toeplitz compressed sensing matrices with applications to sparse channel estimation," IEEE Trans. Inf. Theory, Nov. 2010.

[14] M. Mishali and Y. C. Eldar, "From Theory to Practice: Sub-Nyquist Sampling of Sparse Wideband Analog Signals", IEEE J. Sel. Top. Sign. Process., vol. 4, no. 2, pp. 375-391, Apr. 2010.

[15] M. Mishali, et al., "Xampling: Analog to Digital at Sub-Nyquist Rates", IET Circuits, Devices & Systems, vol. 5, no. 1, pp. 8–20, Jan. 2011.

[16] H. Rauhut, J. Romberg, and J. Tropp, "Restricted isometries for partial random circulant matrices," Appl. Comput. Harmon. Anal., May. 2011.

[17] P. Boufounous and R. Baraniuk, "1-bit compressive sensing," in Proc. Conf. Inform. Science and Systems (CISS), Mar. 2008.

[18] L. Jacques et al., "Robust 1-bit compressive sensing via binary stable embedding of sparse vectors," submitted, 2011.

[19] D. Lee et al., "Combined Nyquist and compressed sampling method for radio wave data compression of a heterogeneous network system," IEICE Trans. Commun., vol. E93-B, no. 12, pp. 3238-3247, Dec. 2010.

[20] D. Lee et al., "Flexible wireless system: Unified wireless platform for a wide variety of wireless systems," in Proc. ICST CrownCom, Jun. 2011.

[21] H. Shiba, Y. Yamaguchi, K. Akabane, T. Yamada, and K. Uehara, "A flexible wireless system supporting for a wide variety of wireless systems," IEICE Technical Report, SR2010-37, Jul. 2010.

[22] M. Kawashima, Y. Yamaguchi, K. Nishikawa, and K. Uehara, "Broadband low noise amplifier with high linearity for software-defined radios," Proc. European Microwave Integrated Circuit Conference (EuMIC) 2007, pp. 243 - 246, Oct. 2007.

[23] T. Kaho, Y. Yamaguchi, H. Shiba, D. Lee, T. Yamada, M. Kawashima, and K. Uehara, "Proposal of a wide-band and high dynamic range receiver for flexible wireless systems," IEICE Tech. Report MW2010-61, Jul. 2010.

[24] T. Yamada, D. Lee, H. Shiba, Y. Yamaguchi, and K. Uehara, "Signal Separation and Reconstruction Method for Simultaneously Received Multi-

System Signals in a Unified Wireless System," Proc. 6th International Conference on Cognitive Radio Oriented Wireless Networks, May, 2011.

[25] D. Lee, T. Yamada, H. Shiba, Y. Yamaguchi, and K. Uehara, "Time-frequency Domain Weighted Measurement Matrix Generation Method for Compressed Sensing," IEICE Society Conference, Sep. 2010.

[26] D. Lee, T. Yamada, H. Shiba, Y. Yamaguchi, and K. Uehara, "Processing burden reduction of a large-scale data compression by employing averaged compressed sensing," IEICE Tech. Report SR2010-69, Jan. 2011.